



ISSN 0975-413X  
CODEN (USA): PCHHAX

Der Pharma Chemica, 2017, 9(7):115-120  
(<http://www.derpharmachemica.com/archive.html>)

## Photocatalytic Degradation of Azo Dye Congo Red Using $\text{Ni}_{0.6}\text{Co}_{0.4}\text{Fe}_2\text{O}_4$ as Photocatalyst

Narde SB<sup>1\*</sup>, Lanjewar RB<sup>2</sup>, Gadegone SM<sup>3</sup>, Lanjewar MR<sup>4</sup>

<sup>1</sup>D.B. Science College, Gondia, Maharashtra 441614, India

<sup>2</sup>Dharampeth M.P. Deo Memorial Science College, Nagpur, Maharashtra 441614, India

<sup>3</sup>Kamla Nehru College, Nagpur, Maharashtra 441614, India,

<sup>4</sup>Department of P.G., RTMNU, Nagpur, Maharashtra 441614, India

---

### ABSTRACT

In the present work the photocatalytic degradation efficiency of the synthesized mixed metal ferrite sample having formula  $\text{Ni}_{0.4}\text{Co}_{0.6}\text{Fe}_2\text{O}_4$  against Congo Red dye in aqueous solution was investigated. The ferrite was prepared via sol-gel auto combustion route at pH 7 and annealed at 800°C. It was characterized using XRD, FTIR, SEM-EDS techniques. Structural characterization by X-ray diffraction studies confirms the formation of nano ferrite with cubic spinel structure. The photo catalytic experiments were carried out in presence of short wave UV light for 100 ml dye solution with respect to effect of pH, catalyst loading, different dye concentration and the influence of these parameters on photo degradation of dye was studied for contact time 120 min. The photo degradation efficiency of ferrite was found to be maximum at pH 3 for 0.3 g ferrite for 100 ml of 10 mg/l dye solution.

**Keywords:** Auto-combustion, Congo red, Ni-Co nanoferrites, Photocatalytic degradation

---

### INTRODUCTION

Environmental problems related with organic pollutants promote the development of elementary and applied research in the area of environment [1]. Among them synthetic dyes such as azo dyes containing -N=N- group are the major industrial pollutants and water contaminants [2]. These dyes are widely used in the textile industry for dyeing nylon, cotton, wool and silk. Waste water from these industries has caused a severe problem to the environment. The discharged wastes containing azo dyes are toxic to microorganisms, aquatic life and also for human beings [3]. The degradation of azo dyes in industrial wastewater is therefore a point of concern. In recent years, semiconductor-assisted photo-catalysis has come up as a promising tool to substitute the traditional wastewater treatment. It has fascinated the public concern for its ability to convert the pollutants into the harmless substances directly in the waste water [4]. Moreover, it is cost effective, highly efficient, low energy-consumption, moderate condition, extensive applicability and decreases secondary pollution [5]. For the present study, Congo Red, an azo dye is selected to investigate photocatalytic efficiencies of newly synthesized ferrite sample prepared by sol gel auto combustion method [6-8].

### EXPERIMENTAL

#### Materials

AR grade iron nitrate nonahydrate ( $\text{Fe}(\text{NO}_3)_3 \cdot 9\text{H}_2\text{O}$ ), Nickel nitrate hexahydrate ( $\text{Ni}(\text{NO}_3)_2 \cdot 6\text{H}_2\text{O}$ ), Cobalt nitrate hexahydrate ( $\text{Co}(\text{NO}_3)_2 \cdot 6\text{H}_2\text{O}$ ), citric acid, liquor ammonia and Congo red dye, high purity of 99.99% and used without further purification.

#### Method

##### Synthesis of ferrite

Ferrite Nanoparticles with compositional formula  $\text{Ni}_{0.6}\text{Co}_{0.4}\text{Fe}_2\text{O}_4$  were synthesized by sol gel auto-combustion method [9]. The above mentioned metal ion precursors and citric acid (molar ratio 1:1) were weighed in desired stoichiometric proportions, dissolved separately in minimum amount of distilled water, then mixed together with constant stirring and the pH value of the solution was adjusted to 7 using aqueous ammonia solution. The solution was then slowly heated and stirred on a hot plate magnetic stirrer at 80°C till gel was formed which was ignited and burnt in a self-propagating combustion manner to obtain loose powder. The powder was finally annealed at 800°C in a muffle furnace for 2 h.

### Characterization of Ni<sub>0.6</sub>Co<sub>0.4</sub>Fe<sub>2</sub>O<sub>4</sub> nanoparticles

Structural characterization of the prepared samples were carried out by X-ray diffraction studies using Bruker AXS, D8 Advance spectrophotometer with Cu-K $\alpha$  radiation ( $\lambda=1.5418 \text{ \AA}$ ) in a wide range of Bragg's angle (20-80°C) at room temperature. Infrared spectra of the powder samples were recorded using Fourier Transform Infra-Red Spectrophotometer (FTIR Nicolet, Avatar 370 model) by the KBr pellet method. The microstructure of the powder samples was investigated using Scanning Electron Microscope (SEM) (JEOL Model JSM-6390LV). Elemental analysis was carried out by using Energy Dispersive Spectrometer (EDSA) (JEOL Model JED-2300). UV-Visible spectroscopic study is performed with Shimadzu UV1800 spectrophotometer.

### Photocatalytic activity

Photo degradation study for Congo red (synonyms-C.I. Direct red28, Cotton red.C.I.22120, molecular weight=696.67 g/mol<sup>-1</sup>, C<sub>32</sub>H<sub>24</sub>N<sub>6</sub>O<sub>6</sub>S<sub>2</sub>.2Na) was performed by batch experiments. Photo degradation experiments were carried out in presence of short wavelength UV light (254 nm). Cobalt substituted nickel ferrite with compositional formula Ni<sub>0.6</sub>Co<sub>0.4</sub>Fe<sub>2</sub>O<sub>4</sub> is used as Photocatalyst. 100 mg/l standard dye stock solution was prepared by dissolving Congo red in double distilled water and suitable dilutions were made for further study. For each experiment 100 ml of dye solution is used. The pH of the dye solution was adjusted using 0.1 N HCl and 0.1 N NaOH solution using digital pH meter. The dye solution was stirred well as well as aerated and 5 ml samples were withdrawn at regular time interval of 30 min, centrifuged for 5 min to remove photo catalyst completely and absorbance was measured using Shimadzu UV1800 spectrophotometer. The photo degradation experiments have been conducted three times to minimize error and average values are reported. The percentage degradation was calculated by using the formula:

$$\text{Percentage degradation} = \{(A_0 - A_t) \div A_0\} \times 100$$

Where, A<sub>0</sub> is the initial absorbance of the dye solution, A<sub>t</sub> is the absorbance at time interval 't'.

## RESULT AND DISCUSSION

### Characterization of ferrite

#### X-Ray Diffraction (XRD) studies

X-ray diffraction pattern of Ni<sub>0.6</sub>Co<sub>0.4</sub>Fe<sub>2</sub>O<sub>4</sub> ferrite system shown in the Figure 1 confirms the formation of single phase cubic spinel structures. The corresponding analytical data for the most intense peak at (311) plane is shown in Table 1. All the planes shown in XRD pattern were indexed using Bragg's law. All the characteristic peaks corresponding to the characteristic planes at their respective 2 $\theta$  values were matched with JCPDS standard powder diffraction card No.742081 having space group Fd3m (227). Most intense peak (311) at 35.70° was used to calculate crystallite size using Debye Scherer's formula [10] given by:

$$D_{hkl} = 0.9 \lambda / \beta \cos \theta$$

Where, D<sub>hkl</sub> is the crystallite size,  $\lambda$  is wavelength of the X-ray radiation,  $\beta$  is the full width at half maximum (FWHM) of the most intense diffraction peak and  $\theta$  is Bragg's angle. The average crystallite size of the ferrite samples was found to be 57.12 nm. The lattice parameter of the sample was found to be 8.332 Å.

**Table 1: Values of crystallite size, lattice parameter (a), d-spacing (d), X-ray density (dx) of nano ferrite with 2 $\theta$ (degrees) and  $\beta$  (degrees) (FWHM)**

S. No.	2 $\theta$ (degrees)	$\beta$ (degrees) (FWHM)	d-spacing (Å)	Crystallite size (nm)	Lattice Parameter in Å (a)	X-ray density (dx) (g/cm <sup>3</sup> )	Volume of unit cell (V) (Å <sup>3</sup> )
1	35.60	0.255	2.51998	57.12	8.357	5.472	583.696

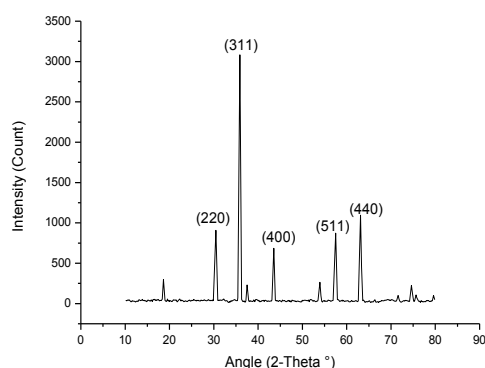


**Figure 1: XRD spectrum of ferrite sample**

#### Fourier Transform Infrared Spectroscopy (FTIR) studies

The spinel structure of the annealed nano ferrite sample is supported by FT-IR spectrum of the sample shown in Figure 2. The FT-IR transmission spectra of cobalt substituted nickel ferrites show two dominant absorption bands  $\nu_1$  and  $\nu_2$  in the range of 400-600 cm<sup>-1</sup> indicating presence of M-O stretching vibration band, the characteristic peak of the spinel structure.

These bands are very sensitive to changes in interaction between oxygen and cations in octahedral and tetrahedral positions [11]. The high frequency band at  $576\text{ cm}^{-1}$  is assigned to stretching vibrations of the tetrahedral groups and lower frequency band near  $400\text{ cm}^{-1}$  is attributed to the stretching mode of the octahedral M-O groups in the ferrites. The difference in positions of frequency bands is due to the difference in the  $\text{Fe}^{3+}$ -O distance for octahedral and tetrahedral complexes.

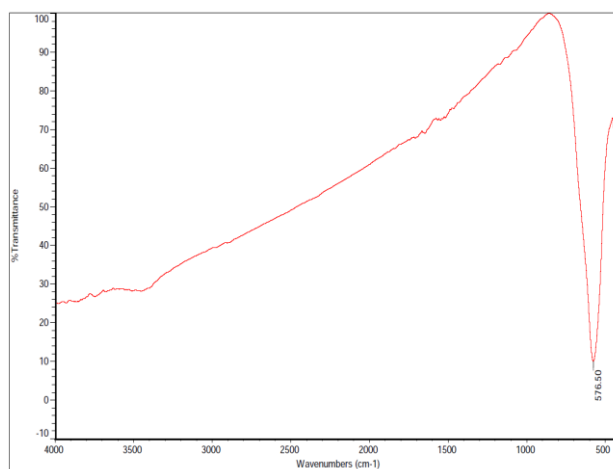


**Figure 2: Fourier transform infrared spectroscopy spectrum of ferrite sample**

### Scanning Electron Microscopy (SEM) studies

SEM image of cobalt substituted nickel nano ferrites is shown in Figure 3. SEM micrograms show formation of largely agglomerated well defined nano particles of sample with high porosity. Moreover, the voids and pores present in the samples are attributed to the release of large amount gases during combustion process.

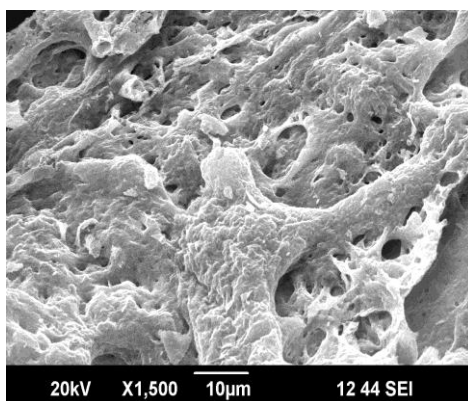


**Figure 3: Scanning electron microscopy image of ferrite**

### Elemental analysis by Energy Dispersive Spectrometer (EDS)

The elemental analysis of ferrite system is analyzed by an EDS and the elemental % and atomic % of various elements in the samples are shown in Table 2.

**Table 2: Energy dispersive spectrometer data for ferrite system**

Element	(keV)	Mass%	Atom%	K
O K	0.525	12.25	33.11	0.4247
Fe K	6.398	61.45	47.57	1
Co K	6.924	13.96	10.24	1.1651
Ni K	7.471	12.34	9.08	1.2976
Total	-	100	100	-

Figure 4 shows the EDS pattern obtained for sample  $\text{Ni}_{0.6}\text{Co}_{0.4}\text{Fe}_2\text{O}_4$  which gives the elemental and atomic composition in the sample. The compounds show the presence of Ni, Co, Fe and O without precipitating cations.

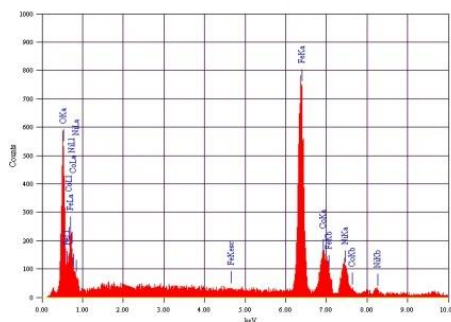


Figure 4: Energy dispersive spectrometer pattern of ferrite

### Photo degradation of Congo red

The photocatalytic degradation efficiency of the synthesized sample against Congo red dye in aqueous solution was investigated in presence of short wave UV light for 100 ml dye solution and the influence of following parameters on degradation was studied.

#### Effect of pH on photo degradation of Congo red

pH of the solution plays an important role in controlling the adsorption and photo degradation of dye on to catalyst surface. To determine the optimum pH conditions for the photo degradation of Congo red, the effect of pH was studied over the pH range of 3-10, with a stirring time of 30 min. Here the initial concentrations of dye and catalyst dosage were set at 10 mg/l and 0.1 g respectively, for all batch tests in this experiment. The pH value of Congo red solution was adjusted using 0.1 N HCl and 0.1 N NaOH. The results obtained are presented in Figure 5. It was observed that at pH 3 the photocatalyst shows maximum photocatalytic activity. pH 2 is avoided because Congo red dye sediments rapidly at pH 2 with increasing dye concentration. This observation is also supported by isoelectric point value of Congo Red which is pH 3 [12,13]. The photo degradation efficiency of the ferrite was found to be maximum for pH 3 (40.28%) and decreases gradually up to pH 10 (15.45%). Hence, all the succeeding investigations were performed at pH 3 Figures 6 and 7.

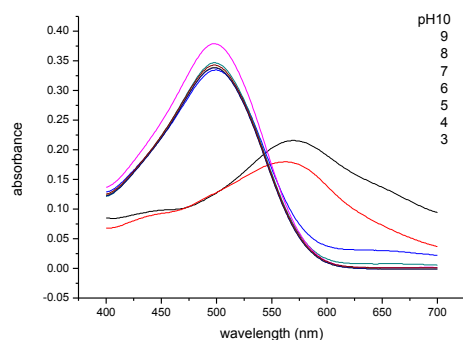


Figure 5: UV/VIS spectra of CR solution at different pH

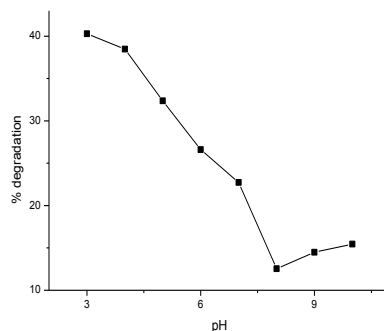


Figure 6: Variation in % degradation of CR solution w.r.t. pH for 120 min time of irradiation using  $\text{Ni}_{0.4}\text{Co}_{0.6}\text{Fe}_2\text{O}_4$

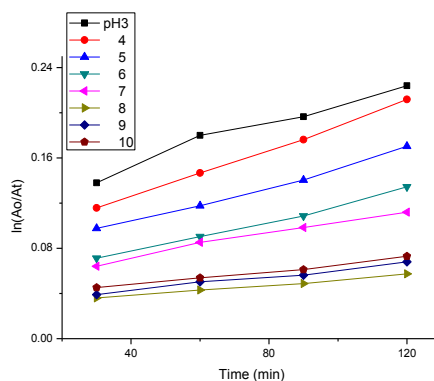


Figure 7: Degradation kinetics of CR solution w.r.t. pH for 120 min time of irradiation using  $\text{Ni}_{0.4}\text{Co}_{0.6}\text{Fe}_2\text{O}_4$

#### Effect of catalyst loading on photo degradation of Congo red

The effect of photocatalyst loading was investigated by adding various amounts of catalyst in the range of 0.05-0.3 g into the beaker containing 100 ml of 10 mg/l dye solution at pH 3, for all batch experiments. The removal of Congo red at different doses is shown in Figures 8 and 9. It was found that with the increase in catalyst dosage the removal percentage of dye increases. At equilibrium, the percentage of dye removal was increased from 19.45-66.08% with the increase of catalyst doses from 0.05-0.3 g, respectively. The increase in percentage of dye removal with increasing catalyst dosage is due to increase of sorption active sites at the catalyst surface as the extent of adsorption is directly proportional to the adsorption sites which is nothing but the amount of dosage [14]. Consequently, the catalyst dose was maintained at 0.2 g for further experiments, which was considered to be sufficient for the removal of Congo red.

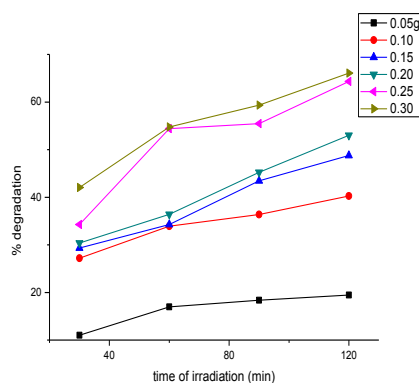


Figure 8: Variation in % degradation of CR solution w.r.t. ferrite concentration for 120 min time of irradiation

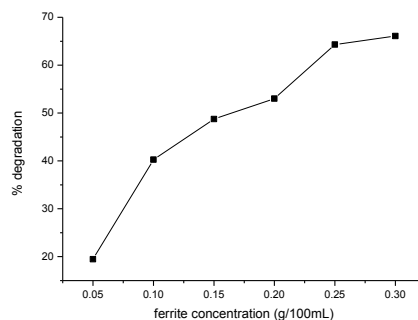


Figure 9: Variation in % degradation of CR solution w.r.t. ferrite concentration for 120 min time of irradiation

#### Effect of initial dye concentration on photo degradation of Congo red

The photo degradation is greatly influenced by the concentration of the dye solution, as the rate photo degradation reaction is directly proportional to the concentration of the solute [15]. To determine the percentage of photo degradation of Congo red, as a function of initial dye concentration, we have carried out batch experiments, taking 0.2 g of catalyst in 100 ml dye solution, for 2 h contact time, at pH 3. The concentration of Congo red solution was varied from 10-50 mg/l maintaining same experimental conditions. It is clear from Figure 10 those removal percentages of the Congo red dye is high at lower concentration and comparatively decreases with increase in dye concentration. The percentage of dye removal was found to decrease from 53% at 10 mg/l dye solution to 13.97% at 50 mg/l.

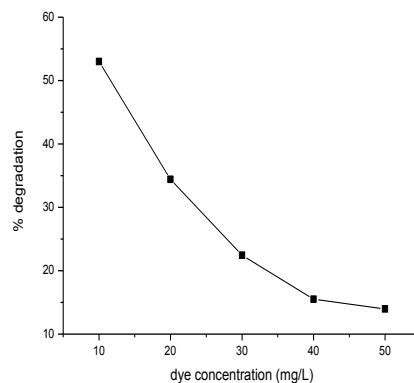


Figure 10: Variation in % degradation of CR solution w.r.t. dye concentration for 120 min time of irradiation for ferrite

### CONCLUSION

Cobalt substituted nickel nano ferrite with compositional formula  $\text{Ni}_{0.6}\text{Co}_{0.4}\text{Fe}_2\text{O}_4$  was successfully prepared by sol gel auto combustion method and characterized by XRD, FTIR, SEM-EDS spectroscopic techniques and it was successfully employed to photocatalytic degradation of Congo Red in the presence of short wave UV light for 100ml dye solution with respect to effect of pH, catalyst loading and different dye concentrations. It is found that the synthesized cubic spinel ferrite sample shows maximum photocatalytic activity of 40.28% at pH 3 for 100 ml of 10 mg/l Congo red dye solution for 0.1 g ferrite and with increase in catalyst concentration it reaches to 66.08% for 0.3 g ferrite. Also the photocatalytic activity was found to decrease with CR concentration from 53% at 10 mg/l to 13.97% at 50 mg/l dye solution for 0.2 g ferrite per 100 ml dye solution.

### ACKNOWLEDGEMENTS

Author SBN is thankful to the STIC, Cochin, Principal, Kamala Nehru Mahavidyalaya, Nagpur, Principal, D.B. Science College, Gondia for providing necessary laboratory facilities.

### REFERENCES

- [1] M. Ahmad, R. Alrozi, *Chem. Eng. J.*, **2011**, 510-516.
- [2] A.V. Salker, S.D. Gokakakar, *Int. J. Phys. Sci.*, **2009**, 377-384.
- [3] U.G. Akpan B.H. Hameed, *J. Hazard. Mater.*, **2009**, 170(2-3), 520-529.
- [4] M. Kulkarni P. Thakur, *Int. J. Eng. Res. Gen. Sci.*, **2014**, 2, 245-254.
- [5] K. Yogendra, S. Naik, K.M. Mahadevan, N. Madhusudhana, *Int. J. Environ. Sci. Res.*, **2011**, 1(1), 11-15.
- [6] F. Deganello, G. Marci, G. Deganello, *J. Eur. Ceram. Soc.*, **2009**, 29 439-450.
- [7] S. Khorrani, A.A. Mehrdad, Sharif, M. Abdizadeh, *Middle East J. Sci. Res.*, **2012**, 11(9), 1202-1206.
- [8] S. Bhukal, T. Namgyal, S. Mor, S. Bansal S. Singhal, *J. Mol. Struct.*, **2012**, 1012, 162-167.
- [9] S. Naraavula, V. Katrapally, *World. J. Nano. Sci. Eng.*, **2015**, 5, 140-151.
- [10] A.K.M.A. Hossain, M.L. Rahman, *J. Magn. Magn. Mater.*, **2011**, 323(15), 1954-1962.
- [11] P. Shankar, Bhavyashri, R.S. Raveendra, A. Jayasheelan, *Int. J. Adv. Sci. Tech. Res.*, **2015**, 1(5).
- [12] R. Ahmad, R. Kumar, *Appl. Surf. Sci.*, **2010**, 257, 1628-1633.
- [13] Z. Zhang, L. Moghaddam L, I.M. O'Hara, W.O.S. Doherty, *Chem. Eng. J.*, **2011**, 178, 122-128.
- [14] B. Royer, N.F. Cardoso, E.C. Lima, J.C.P. Vaghetti, N.M. Simon, T. Calvete, R.C. Veses, *J. Hazard. Mater.*, **2009**, 164, 1213-1222.
- [15] X.H. Lu, D.Z. Zheng, J.Y. Gan, Z.Q. Li, C.L. Liang., P. Liu, Y.X. Tong, *J. Mater. Chem.*, **2010**, 20, 7118-7122.